Electronic Supplementary Information

Constructing hyperbranched polymers as stable elastic framework for copper sulfide nanoplates enhancing sodium-storage performance

Aiqiong Qin,[a] Hao Wu,[a] Jie Chen,[a] Ting Li,[a]* Shenghui Chen,[a] Daohong Zhang,[a]* and Fei Xu[b]*

[a] *Key Laboratory of Catalysis and Materials Science of the State Ethnic Affairs Commission & Ministry of Education, College of Chemistry and Materials Science, South-Central University for Nationalities, Wuhan, 430074, P. R. China.*

[b] *School of Power and Mechanical Engineering, Wuhan University, Wuhan 430072, P. R. China.*

Corresponding Author

*Ting Li (liting@mail.scuec.edu.cn)

*Daohong Zhang (zhangdh27@163.com)

*Fei Xu (xufei2058@whu.edu.cn)

Supplementary data: Additional figures and tables as mentioned in the text

1. Synthesis scheme and structure characterization of AHP

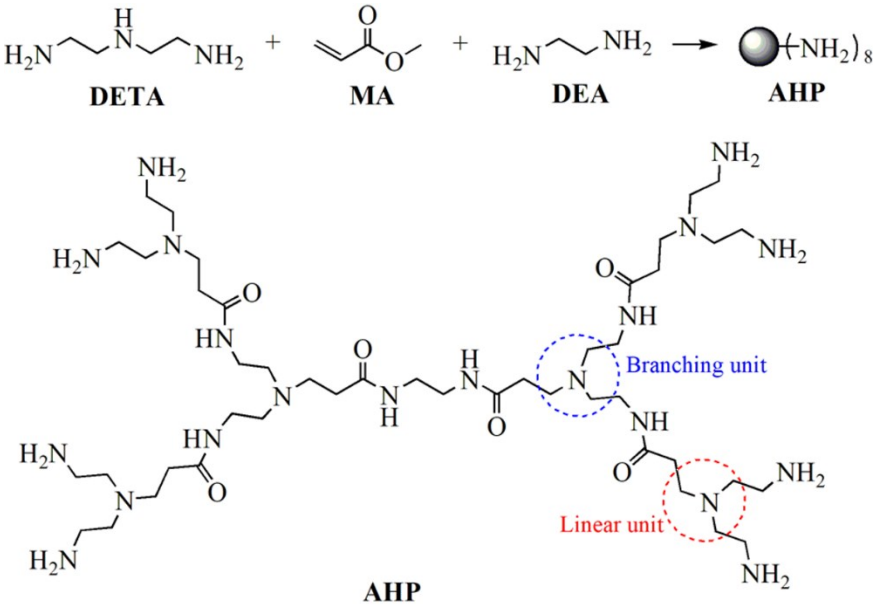

Figure S1. Synthesis scheme and structure of AHP.

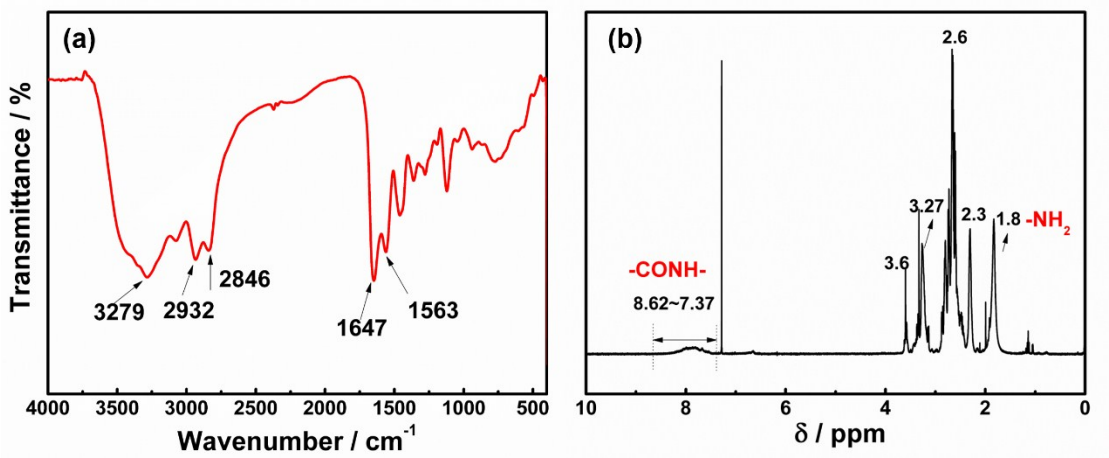

Figure S2. (a) The FT-IR spectra and (b) ^{1}H NMR spectra of AHP.

Figure S2a shows main absorption peaks include 3279 cm^{-1} (s, N-H), 2932 cm^{-1} and 2846 cm^{-1} (s, C-H), 1647 cm^{-1} (s, C=O), and 1563 cm^{-1} (b, C-N). Figure S2b shows chemical shifts include 8.62-7.37 ppm (m, 1H, -CONH-), 3.60 ppm (s, 2H, -$NHCH_2CH_2NH$-), 3.27 ppm (s, 2H, -$COCH_2CH_2$-), 2.6 ppm (ddt, 4H, -NCH_2CH_2N-), 2.3 ppm (s, 2H, -$COCH_2CH_2$-), and 1.8 ppm (s, 2H, -NH_2).

2. Thermogravimetric (TG) analysis of AHP, Cu_9S_5-AHP and Cu_9S_5 NP

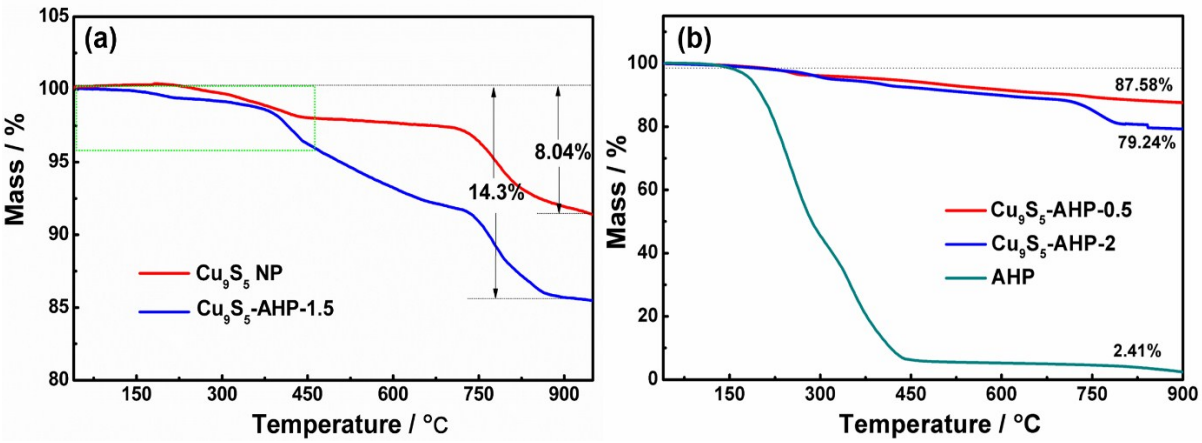

Figure S3. TGA curves of (a) Cu_9S_5 NP and Cu_9S_5-AHP-1.5, (b) AHP, Cu_9S_5-AHP-0.5 and Cu_9S_5-AHP-2 in N_2 atmosphere at a heating rate of 10 °C min^{-1}

3. FT-IR and Raman characterization of Cu_9S_5-AHP-1.5

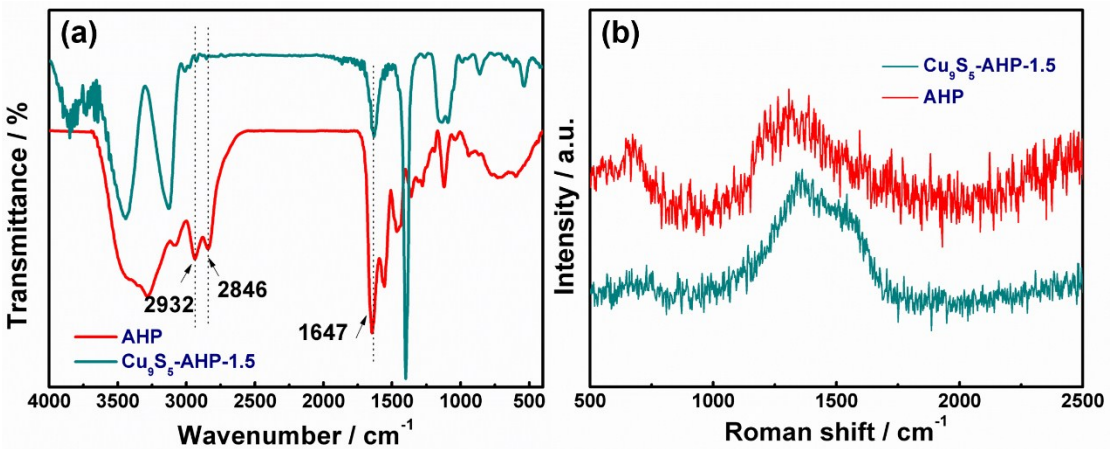

Figure S4. FT-IR (a) and Raman (b) spectra of Cu_9S_5-AHP-1.5 and AHP.

The presence of AHP is confirmed by IR peaks at 2932, 2846, and 1647 cm^{-1}, and Raman bands at ~1350 and ~1500 cm^{-1}.

4. ICP-OES analysis of Cu_9S_5-AHP-1.5 sample

Table S1 The results of ICP-OES analysis of Cu_9S_5-AHP-1.5 sample.

Element	Concentration (mg L^{-1})
Cu	**57.26**
S	**17.98**

atomic ratio of Cu/S = 1.59:1

5. Na-storage performances of Cu_9S_5 NP, Cu_9S_5-AHP and AHP electrodes.

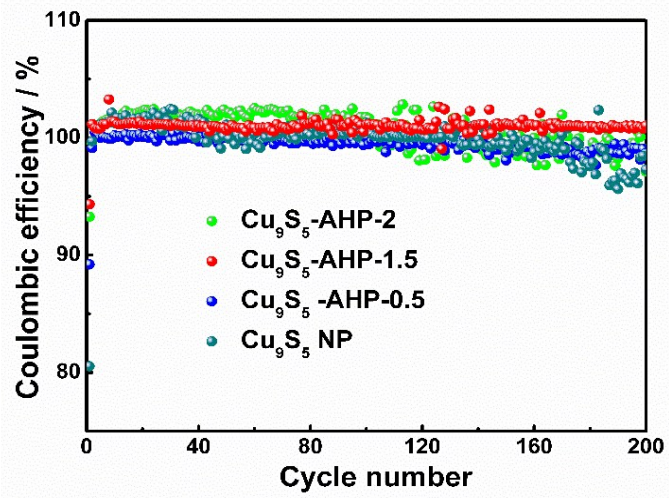

Figure S5. Coulombic efficiency in 1 M $NaPF_6$ + DOL-DME (1:4 by volume) at 100 mA g^{-1}

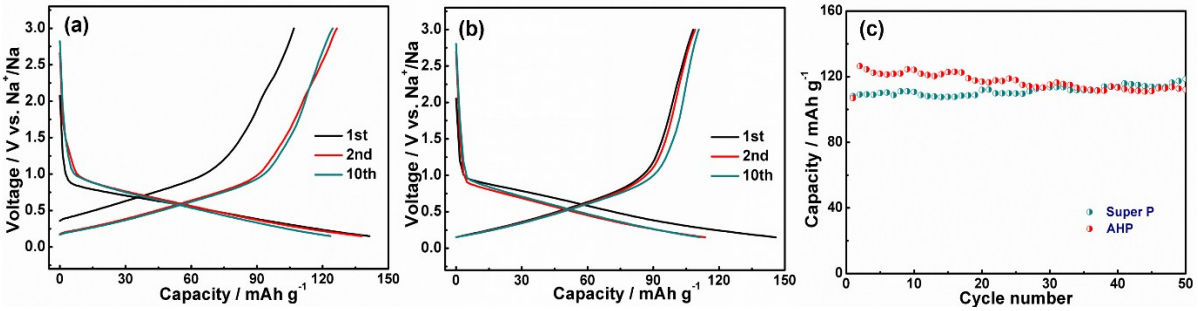

Figure S6 Charge/discharge curves of (a) AHP and Super P (1:1), (b) Super P and cycling performance (c) at 100 mA g^{-1}.

The specific capacities are calculated based on the mass of Super P only to illustrate the contribution of AHP. The AHP and Super P (1:1) electrode delivers a reversible capacity of ~120 mAh g^{-1}, while the that for Super P electrode is ~110 mAh g^{-1}. Therefore, the capacity of AHP is estimated to be about 20 mAh g^{-1}.

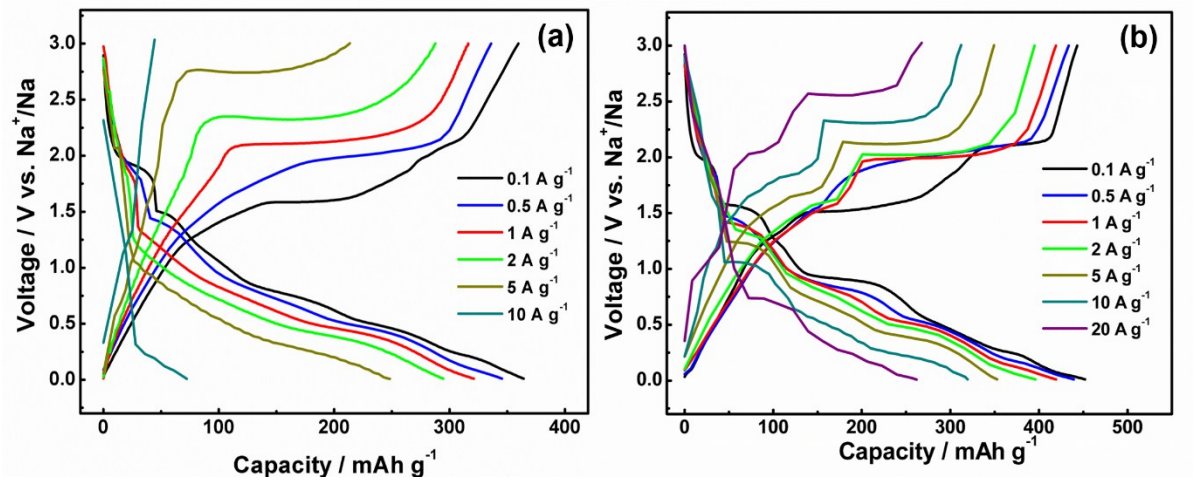

Figure S7. Charge/discharge curves of (a) Cu_9S_5 NP and (b) Cu_9S_5-AHP-1.5 at various current densities.

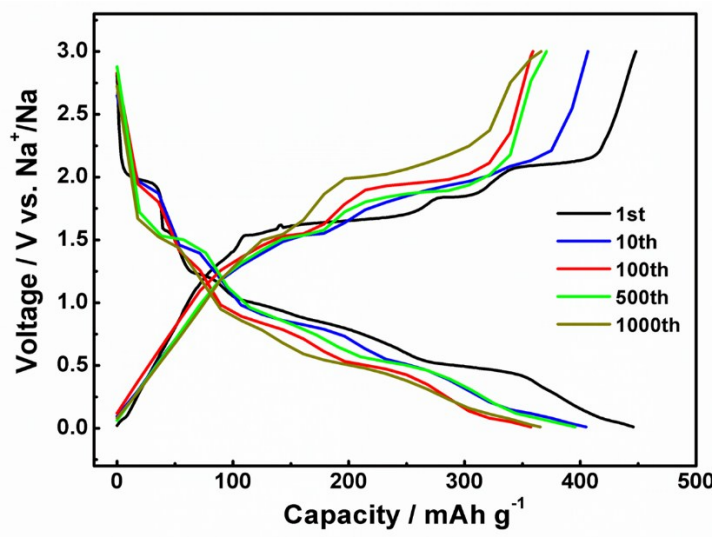

Figure S8. Discharge/charge profiles of Cu_9S_5-AHP-1.5 at 1000 mA g^{-1}.

6. The morphologies of Cu_9S_5-AHP-1.5 and Cu_9S_5 NP electrodes before and after cycling

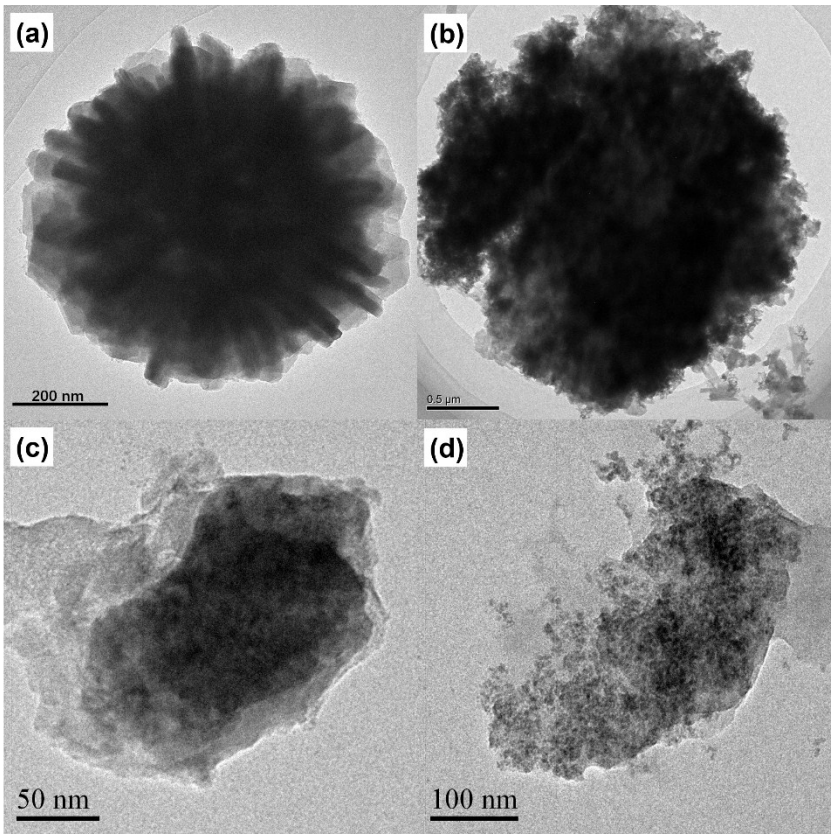

Figure S9. TEM images of Cu_9S_5-AHP-1.5 (a) at initial state, (b) after 300 cycles and Cu_9S_5 NP (c) at initial state, (d) after 300 cycles at 100 mA g^{-1}.

7. Comparison of the results in this study with those of previously reported in the literatures.

Table S2 Comparison of the results in this study with those of previously reported in the literatures.

Materials	electrolyte	Voltage range (V)	Current density (mA g^{-1})	Initial capacity (mAh g^{-1})	Cycles/ Retained capacity (mAh g^{-1})	ref
Cu_9S_5-AHP-1.5	$NaPF_6$-DOL/DME	0.01~3.0	100	459.5	200/412.9	This work
			1000	445.9	1000/365.6	
$Cu_{1.8}S$	$NaCF_3SO_3$-DEGDME	0.1~2.2	84	~330	50/~250	1
		0.5~2.2	84	~200	50/~260	1
		0.7~2.2	84	~110	50/~130	1
		0.5~2.2	840	~150	1000/~240	1
Cu_9S_5	$NaClO_4$-EC/PC	0.01~3.0	100	412	200/344.3	2
CuS	$NaPF_6$- DME	1.0~3.0	31	348.6	100/41.8	3
CuS(S48)	$NaClO_4$- DME	0.3~2.2	5000	132.6	5000/132	4
Cu_2S	$NaCF_3SO_3$-TEGDME	0.4~2.6	50	294	20/261	5
CuS-NDs	$NaPF_6$- DEGDME	0.01~2.7	100	610	500/300	6
CuS	$NaClO_4$-TEGDME	0.1~3.0	50	~475	50/~5	7
		0.6~3.0	50	~410	50/~170	7
		0.7~3.0	50	~200	50/~80	7
	$NaClO_4$-EC/DEC	0.6~3.0	50	~360	50/~0	7
CuS	$NaCF_3SO_3$-DEGDME	0.4~2.6	100	400	50/311.8	8
CuS-RGO-1	$NaCF_3SO_3$-DEGDME	0.4~2.6	100	494.2	50/381.7	8
			1000	345.7	450/~340	8
CuS-RGO-2	$NaCF_3SO_3$-DEGDME	0.4~2.6	100	509.1	50/392.9	8
CuS-RGO-3	$NaCF_3SO_3$-DEGDME	0.4~2.6	100	432.5	50/328.9	8
Cu_2S	$NaPF_6$-DME	0.01~2.5	5000	317	5000/~280	9

8. Electrochemical impedance spectra (EIS) analysis of Cu_9S_5-AHP-1.5 and Cu_9S_5 NP at initial state and the full charge state after 100 cycles

Table S3 Simulation results of the EIS using the equivalent circuit.

Cycle	Cu_9S_5 NP		Cu_9S_5-AHP-1.5	
	R_{SEI}(Ω)	R_{ct} (Ω)	R_{SEI} (Ω)	R_{ct} (Ω)
Before	26.49	334.5	8.7	113.9
100th Cycle	0.657	1078	0.01	3.2

R_{SEI} and R_{ct} are the resistances of solid electrolyte interface (SEI) film and charge transfer, respectively.

9. Cyclic voltammetry analysis of Cu_9S_5 electrodes and relationship of peak current (i_p) with square root of scan rate ($v^{1/2}$) and scan rate (v), respectively

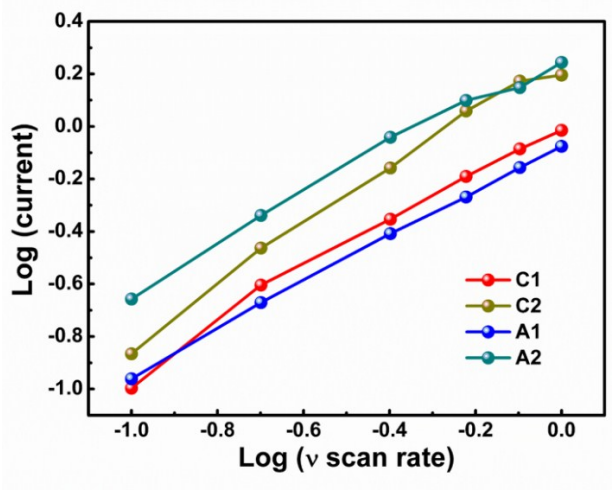

Figure S10. Log(i) vs log(v) plots for different redox peaks of Cu_9S_5-AHP-1.5 electrode.

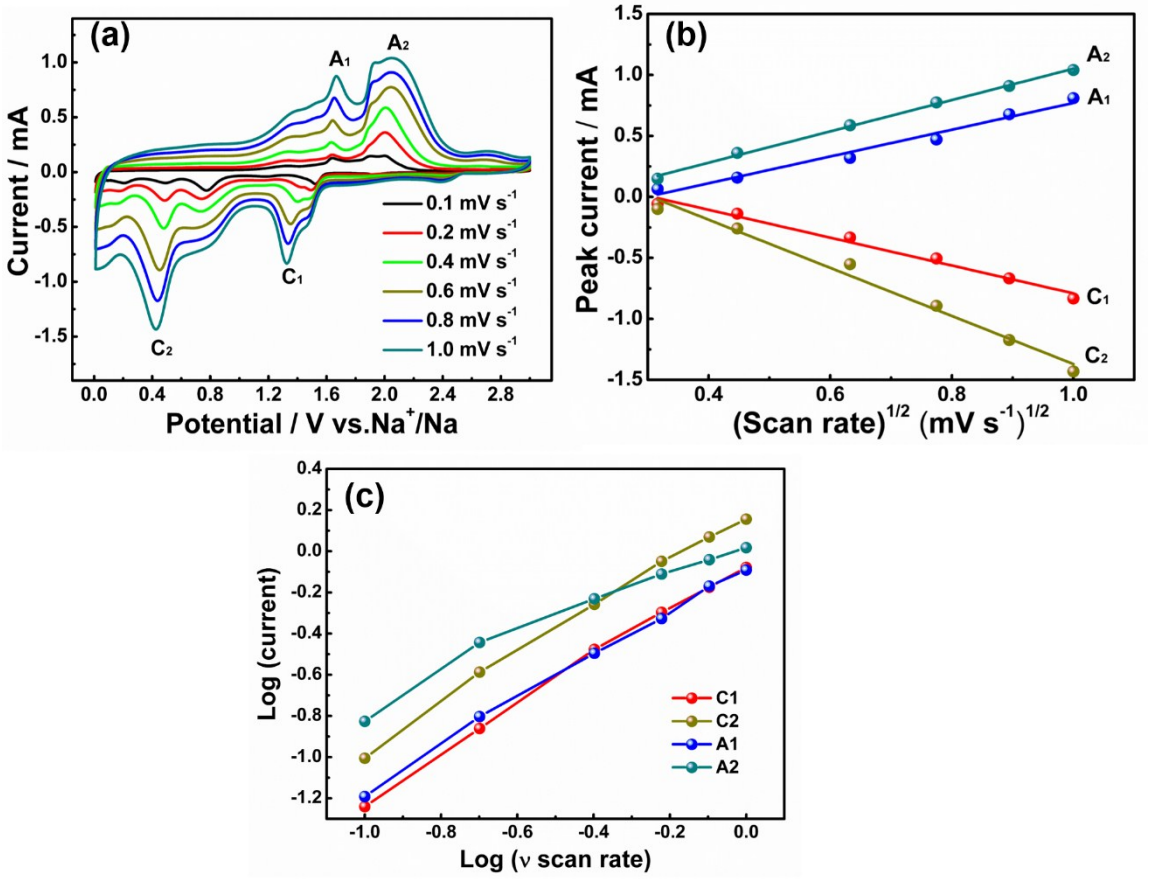

Figure S11. (a) CV curves at different scan rates, (b) linear relationship between peak current (i_p) and square root of scan rate ($v^{1/2}$), (c) Log(i) vs log(v) plots for different redox peaks of Cu_9S_5 NP electrode.

10. Calculation of Na^+ diffusion coefficient of Cu_9S_5-AHP-1.5 and Cu_9S_5 NP from CV

Table S4 The results of diffusion coefficient of Na^+ calculated by CV.

	Cu_9S_5-AHP		Cu_9S_5	
peak	$i_p/v^{1/2}$	**D（$\times 10^{-9}$ cm^2 s^{-1}）**	$i_p/v^{1/2}$	**D（$\times 10^{-10}$ cm^2 s^{-1}）**
C1	0.0401	1.602	0.0361	6.707
C2	0.0714	0.2956	0.0624	1.078
A1	0.0342	0.2170	0.0347	0.8515
A2	0.0698	5.730	0.0406	6.183

The diffusion coefficient of Na^+ is calculated by the following equation (S1):[10,11]

$$i_p=2.69\times10^5 n^{3/2} A D^{1/2} v^{1/2} C_0 \quad (1)$$

where i_p is the peak current (A), n is the number of electrons per molecule during the reaction, A is the contact area between the electrode and electrolyte, D is the diffusion coefficient of Na^+ (cm^2 s^{-1}), C_0 is the concentration of Na^+ ion in the electrode material, and v is the scan rate (V s^{-1}).

11. A single GITT titration and the corresponding linear behavior of *E* vs. $\tau^{1/2}$ relationship

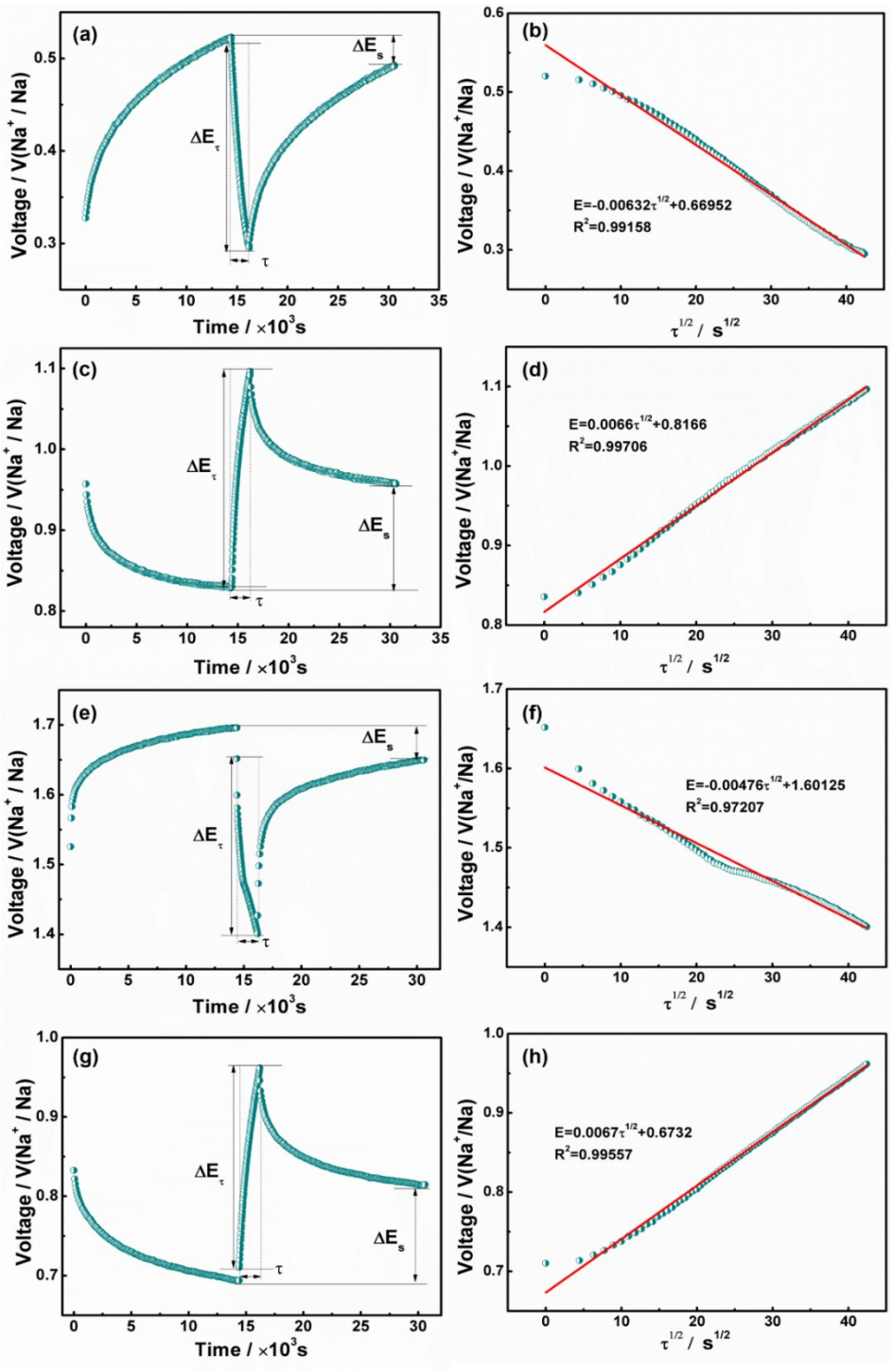

Figure S12. A single GITT titration and the corresponding linear behavior of *E* vs. $\tau^{1/2}$ relationship: (a, b) Cu_9S_5-AHP-1.5 during discharge processes; (c, d) Cu_9S_5-AHP-1.5 during charge processes; (e, f) Cu_9S_5 NP during discharge processes; (g, h) Cu_9S_5 NP during charge processes.

12. N_2 adsorption–desorption isotherm of Cu_9S_5-AHP-1.5 and Cu_9S_5 NP

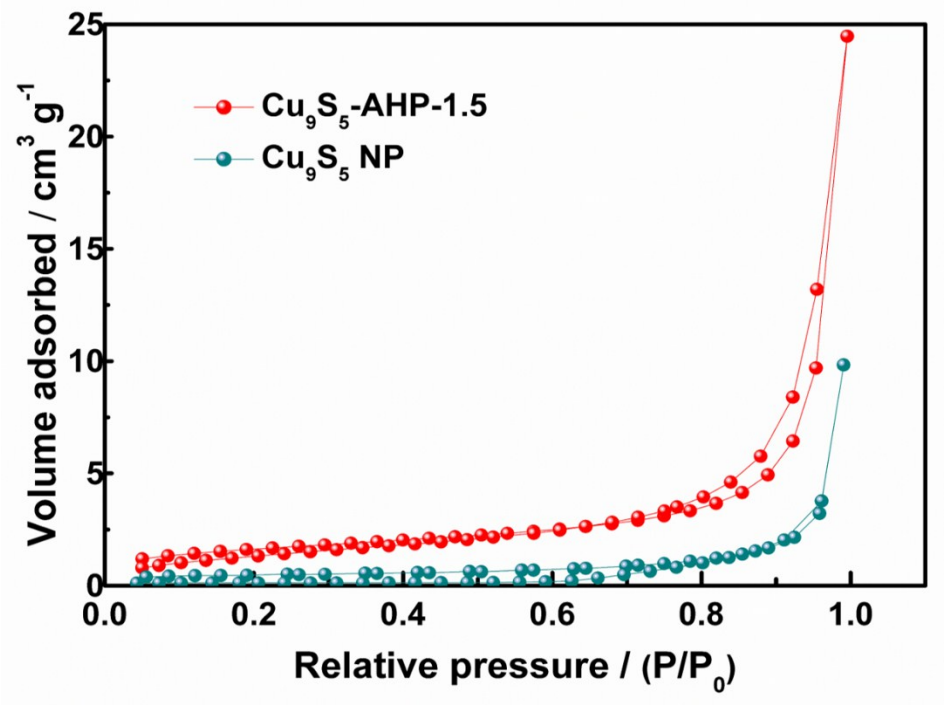

Figure S13. N_2 adsorption-desorption isotherm curves of Cu_9S_5-AHP-1.5 and Cu_9S_5 NP. The specific surface areas of Cu_9S_5-AHP-1.5 and Cu_9S_5 NP are 5.73 and 1.58 $m^2 g^{-1}$, respectively.

13. Calculation of Na^+ diffusion coefficient of Cu_9S_5-AHP-1.5 and Cu_9S_5 NP from CV and GITT

Table S5 The results of diffusion coefficient of Na^+ calculated by CV and GITT

	Cu_9S_5-AEHPA ($\times 10^{-9}$ cm^2 s^{-1})				Cu_9S_5 ($\times 10^{-10}$ cm^2 s^{-1})			
	C1	**C2**	**A1**	**A2**	**C1**	**C2**	**A1**	**A2**
CV	1.602	0.2956	0.2170	5.730	6.707	1.078	0.8515	6.183
GITT	1.647	0.4136	0.7737	1.381	5.354	1.476	0.2665	2.867

References

1 H. Park, J. Kwon, H. Choi, D. Shin, T. Song and X. W. D. Lou, *ACS Nano*, 2018, **12**, 2827-2837.

2 M. Jing, F. Li, M. Chen, J. Zhang, F. Long, L. Jing, X. Lv, X. Ji and T. Wu, *J. Alloys Comp.*, 2018, **762**, 473-479.

3 B. Shi, W. Liu, K. Zhu and J. Xie, *Chem. Phys. Lett.*, 2017, **677**, 70-74.

4 C. An, Y. Ni, Z. Wang, X. Li and X. Liu, *Inorg. Chem. Front.*, 2018, **5**, 1045-1052.

5 J. Kim, D. Kim, G. Cho, T. Nam, K. Kim, H. Ryu. J. Ahn and H. Ahn, *J. Power Sources*, 2009, **189**, 864-868.

6 N. R. Kim, J. Choi, H. L. Yoon, M. E. Lee, S. U. Son, H. Jin and Y. S. Yun, *ACS Sustain. Chem. Eng.*, 2017, **5**, 9802-9808.

7 H. Li, Y. Wang, J. Jiang, Y. Zhang, Y. Peng and J. Zhao, *Electrochim. Acta*, 2017, **247**, 851-859.

8 J. Li, D. Yan, T. Lu, W. Qin, Y. Yao and L. Pan, *ACS Appl. Mater. Interfaces*, 2017, **9**, 2309-2316.

9 H. Li, K. Wang, S. Cheng and K. Jiang, *ACS Appl. Mater. Interfaces*, 2018, **10**, 8016-8025.

10 Z. Wei, D. Wang, M. Li, Y. Gao, C. Wang, G. Chen and F. Du, *Adv. Energy Mater.*, 2018, **8**, 1801102.

11 Y. Yang, Y. Tang, G. Fang, L. Shan, J. Guo, W. Zhang, J. Zhou, C. Wang, L. Wang, and S. Liang, *Energy Environ. Sci.*, 2018, **11**, 3157-3162.